

PART 2

Rice Straw Smoke Generation System for Controlled Human Inhalation Exposures

B.M. Jenkins¹, J.J. Mehlschau¹, R.B. Williams¹, C. Solomon²,
J. Balmes,² M. Kleinman,³ and N. Smith¹

¹Department of Biological and Agricultural Engineering,
University of California, Davis

²Department of Medicine, University of California, San Francisco

³Department of Community and Environmental Medicine,
University of California, Irvine

Abstract

A unique burner system was designed for the purposes of exposing human subjects to rice straw smoke under highly controlled conditions. The system burns individual straws and has produced particle concentrations up to 900 $\mu\text{g}/\text{m}^3$ in a temperature and humidity controlled exposure chamber. Burner operation is fully automatic and programmable. Ignition is by radiant heating in a manner similar to the field. Particle concentration is controlled by the firing interval between straws and by the ratio of burner outlet flow mixing with the main purified air supplied to the exposure chamber. Steady-state particle concentrations are achieved within 5 minutes from start. Repeatability of particle concentration is excellent at the two exposure levels used, 200 and 500 $\mu\text{g}/\text{m}^3$. Measurements of particle size distributions suggest that approximately 80% of mass is in the size fraction below 1 μm . Although particle concentrations are controlled at target levels with good precision, emission factors are higher than achieved with similar material in wind tunnel and field experiments. Further characterization of particulate matter is needed to determine if higher emission factors are associated with changes in particle composition and morphology that may influence exposure results.

Table of Contents

Table of Contents	2
Table of Figures	3
Introduction.....	5
Exposure chamber	6
Rice straw characteristics	7
Design particle emission factors, straw consumption rates, and related factors	7
Final Design.....	9
System Performance and Smoke Characteristics	11
Fuel consumption and burning times	11
Intermittency in burning and chamber concentrations.....	12
Flow rates and firing intervals	12
Air-fuel ratio	13
Residence times	13
Particle concentrations	13
Particle emission factors.....	13
Transient performance and predictions of the surge and chamber concentrations	15
Average concentrations and firing intervals	18
Summary and Conclusions	18
References	20

Table of Figures

Figure 1. Smoke generation and distribution system. Duct dimensions are given as length x diameter (D) or length x rectangular cross section in meters; volumes in cubic meters.	24
Figure 2. Schematic of the straw storage magazine and burner.....	25
Figure 3. View of burner interior showing straw storage magazine with shuttles and pre-loaded straw. Ignition furnaces are located below the magazine. The smoke hood is situated at the top of the right furnace. The front polycarbonate door has been removed for loading.	26
Figure 4. View of ignition furnaces during operation. Left: showing thermal radiation intensity. Right: at peak flaming after igniting a straw.	27
Figure 5. CO ₂ concentrations and temperatures at burner and surge outlets for a 30 s firing interval with rice straw. The surge outlet temperature rise between 20 and 25 min is caused by turning off the mixing fan during this period. The gas sampling line was moved from the burner outlet to the surge outlet at 10.5 min (simultaneous sampling was not performed).	28
Figure 6. CO ₂ concentration at the burner outlet (actual), surge outlet (actual and predicted), and exposure chamber (predicted) for a single firing cycle. Actual temperatures at the burner and surge outlets also shown. Combustion stages from visual observations shown at top and positioned relative to the temperature profile: I = induction period, F = flaming, S = glowing combustion and smoldering (smoldering period may extend beyond visible limit indicated). Actual surge outlet concentration not simultaneous with burner outlet concentration and shown for illustrative purposes. Lag in sampling system causes concentration profiles to be shifted approximately 4 s in time relative to the temperature profiles.....	29
Figure 7. Straw mass conversion fraction and cumulative conversion estimated from CO ₂ concentrations at burner outlet.....	30
Figure 8. Predicted particle concentrations in surge and exposure chamber from estimates of transient particle concentrations at the burner outlet, 45 s firing interval.	31
Figure 9. Predicted particle concentrations in surge and exposure chamber from estimates of transient particle concentrations at the burner outlet, 140 s firing interval.....	32

Figure 10. Predicted and measured CO concentrations (ppmv) in the exposure chamber for 45 and 140 s firing intervals. CO emission factor used for predictions = 5% dry matter.33

Figure 11. Particle size number distributions for smoke in the exposure chamber with a 45 s firing interval: (a) 2.5 min after starting to fire straw, (b) 4.5 min after starting, (c) steady operation after 6 min, (d) 2.5 min after stopping straw firing, and (e) 6 min after stopping. Also shown are geometric mass mean diameters and total mass concentrations as determined by SMPS for the size interval 20 to 930 nm.34

Figure 12. Cumulative particle mass and mass distributions determined by SMPS (size range 20 to 930 nm) for smoke in the exposure chamber under steady operation with a 45 s firing interval compared with cumulative mass distribution determined by cascade impactor from wind tunnel experiments with rice straw. The chamber distribution (adjusted cumulative mass) aligns with the wind tunnel distribution assuming the SMPS result accounts for 80% of total mass.35

Figure 13. Estimated PM concentrations in the exposure chamber for different emission factors (EF, % dry matter) and firing time intervals.36

Figure 14. Estimated CO concentrations in the exposure chamber for different emission factors (EF, % dry matter) and firing time intervals.37

Figure 15. Estimated CO₂ concentrations in the exposure chamber for different emission factors (EF, % dry matter) and firing time intervals.38

Introduction

Largely as a result of perceived health concerns, California in 1991 enacted legislation (AB 1378) curtailing the field burning of rice straw for disposal, a common agronomic practice.¹ California produces roughly a fifth of US rice, principally on about 200,000 ha in the Sacramento Valley (1 ha = 1 hectare = 2.47 acres). Burning straw following grain harvest is practiced for its low cost and expediency, and also for mitigating rice diseases and weeds in succeeding crop cycles. The practice is by no means limited to California, and open burning of straw occurs in many areas around the world. Burning is also practiced in a number of other crops and for land clearing or maintenance (Jenkins, et al., 1992). Smoke includes both harmful respirable particulate matter and gases, but the actual human health impacts from vegetative burning are not well known. Reports from clinicians and health providers of adverse health effects increase during and following periods of high smoke concentrations, but unlike studies of tobacco smoke inhalation, few direct studies of health impacts from agricultural smoke have been conducted. Exposures to biogenic silica fiber emitted from various rice farming operations, including open burning of straw, have been assessed (Lawson, et al., 1995), and rice straw burning has been linked to incidence of asthma attack, especially in children (Torigoe, et al., 2000; Jacobs, et al., 1997). There have been no previous controlled studies of human exposure to rice straw smoke.

The lack of direct evidence of human respiratory injury from inhalation of rice straw smoke has made attempts to control open burning controversial. The agronomic value of burning is largely undisputed, hence fire has served an essential economic role for this crop. Burning can also help reduce the quantities of herbicides and other chemicals otherwise applied for weed and pest control, thereby reducing other environmental impacts. The desire to eliminate burning, or at least substantially curtail the practice as California has chosen to do, stems in part from nuisance and aesthetic considerations, but most importantly from perceptions of health risks to susceptible populations and the public in general. To test the direct effects of rice straw smoke inhalation on airway inflammation and pulmonary function, the State of California initiated a study of controlled exposures with healthy, asthmatic, and allergic individuals. The project is currently focused on acute effects of inhaled particles, with the hypothesis that exposure to rice straw smoke results in concentration-dependent changes in airway cells. The smoke generation system was designed with the intent to simulate most of the attributes of rice straw smoke from actual field burns.

¹California Assembly Bill 1378, "Connelly-Areias-Chandler Rice straw burning reduction act," 1991. California Senate Bill 318, 1997, extended the deadline for curtailment and provided incentives for the development of non-burning alternatives. In 2001 and beyond the fraction of rice straw allowed for burning is limited to a maximum of 25% under the "safe harbor" clause of AB 1378. Growers must demonstrate potential economic loss in order to obtain permits for burning.

Smoke Generation System Design

Design of the smoke generation system was based on characteristics of the exposure chamber, target particle concentrations, exposure duration, straw characteristics and consumption rates, and the need for system automation with good repeatability. Additional considerations included providing adequate upstream residence times for gas-particle phase equilibrium, especially of polycyclic aromatic hydrocarbons (PAH), maintaining chamber air temperature and relative humidity within typical limits, and supplying sufficient air to maintain high air-fuel ratio such as exists in the field. The system was not designed to match all environmental conditions influencing the properties of rice straw smoke to which urban populations may be exposed. Absent are the effects of sunlight on particles in the atmosphere, and chemical reactions and compositional changes that occur while in the atmosphere for extended periods of time.

Exposure chamber

All human exposures are conducted in a controlled environmental chamber within the Human Exposure Laboratory of the Lung Biology Center, University of California, San Francisco. The chamber measures 2.6 m by 2.6 m by 2.4 m high with a volume of 16.4 m³. Air for the chamber is purified through HEPA and activated carbon filters and conditioned for temperature and relative humidity. Clean air to the chamber is supplied at a rate of 230 L s⁻¹ and is typically maintained at 20°C and 50% relative humidity.

The inlet and exhaust flows are adjusted to produce a slight negative pressure at the exposure chamber to prevent contaminants under study from leaking into the surrounding laboratory, both for reasons of general laboratory safety and with blind exposures to avoid alerting subjects during preparation that smoke is present in the chamber (nose clips are worn during exposure). The smoke is quite easy to detect by odor even at low concentrations. The smoke generation system was designed to quickly bring the chamber atmosphere up to the target particle concentration so that subjects could be prepared without the generator producing smoke, and then exposed without having to wait extended periods of time. The smoke generation system also needed to match particle size distribution (90% or more less than 10 µm) and provide the design particle concentrations under continuous automatic operation and with good precision.

Human subjects are exposed in the laboratory to rice straw smoke at two different nominal particle concentrations. The original target concentrations were 200 and 600 µg m⁻³, with exposures ranging from 30 min to 3 h in duration. By comparison, urban concentrations due to rice straw burning in the Sacramento area occasionally exceed 200 µg m⁻³ for short periods of time (2-3 h). More typically ambient concentrations are controlled through restrictions on burning and other sources to maintain total levels below 50 µg m⁻³. Severe wildfires in adjacent forested regions have sometimes driven ambient concentrations in the

valley urban areas above $900 \mu\text{g m}^{-3}$, but on such days agricultural burning is prohibited. The selected test concentrations for the chamber were intended to be high enough to generate measurable responses in the subjects.

Rice straw characteristics

For these tests, a typical California rice variety was specified for use by the California Air Resources Board (CARB) in consultation with advisors from the rice industry.² The M-202 variety selected is a medium-grain rice accounting for more than half the total production in the state. A number of other conditions were placed on the properties of the straw to be used (fertilization practice, yield, avoidance of contamination from road dust). Moisture content, potassium (K) and chlorine (Cl) concentrations, and stem fraction to be used were not specified, but can also influence the fire behavior and emissions. All straw samples collected for the exposure tests were of fall-harvested straw that had experienced no weathering. Average properties of the straw used in the tests described here are listed in Table 1. The volatile fraction is representative of the mass involved in flaming ignition. Carbonaceous residual (fixed carbon) burns by heterogeneous oxidation during the later, smoldering stages of combustion.

Design particle emission factors, straw consumption rates, and related factors

Rice straw burning in California is regulated both in terms of the time when growers can burn and the method of burning employed. Burning is allowed only on officially declared "burn" days when atmospheric conditions are predicted to be suitable for adequate smoke dispersion with little exposure of the urban populations in Sacramento and other southern valley cities. Total crop area is also limited for any given burn day. Growers are restricted to burning in strip-light or backing (wind-opposed) fires. This is intended to produce lower pollutant emissions than the more rapidly moving heading or wind-aided fires (Goss and Miller, 1973). As the fire propagation speed in purely backing mode is slow, strip-lighting, or igniting along a line into the prevailing wind, is the predominant technique, such that the wind is not entirely opposed to the fire spread direction. Growers are also constrained by straw moisture (less than 12% wet basis) and time of day (normally between 10 a.m. and 4 p.m.). The time of day has been shown to influence the particulate matter (PM) emission factor, largely due to changes in straw and soil moisture content. The 4 p.m. limit for burning is intended to eliminate road visibility problems at night and to avoid burning during the evening as the relative humidity and straw moisture increases, the air temperature decreases, and the atmospheric inversion height declines. For the same moisture content and straw yield, the emission factors depend on the composition of straw and extent of weathering before burning, and the velocity profile and turbulence intensity in the approaching air flow. Natural precipitation

²H.L. Carnahan, Ph.D., to Dr. John Holmes, Chief of the Research Division, California Air Resources Board, 2 July 1998.

leaches alkali, chlorine, and other constituents from the straw (Jenkins, et al., 1996c). Chlorine is a flame inhibitor, and the fire behavior is known to be influenced by Cl concentration in the straw (Jenkins, 1996). Alkali metals are catalysts for pyrolysis (Williams and Horne, 1994) and can influence the rate of release of volatile components involved in flaming and pollutant formation.

Previous simulations of rice straw burning have been conducted in wind tunnels for the purposes of estimating pollutant emission factors (mass of pollutant released per unit mass of fuel burned) under well controlled conditions (Jenkins, et al., 1993; 1994; 1996a; 1996b; Jenkins, 1996; Turn, et al., 1997). Wind tunnel measurements of total particulate matter (PM) emission factors for rice straw burning in backing fires range from 0.063 to 0.856% dry matter with a mean of $0.35 \pm 0.10\%$ (COV = 56%).³ A set of wind tunnel experiments on fall harvested M-202 rice straw burned within a few weeks of harvest yielded a mean emission factor of $0.65 \pm 0.22\%$ (COV = 22%). Generally, more than 90% of PM mass falls within the size fraction having aerodynamic diameter below 10 μm (PM₁₀), and much of this is in the fraction below 1 μm . Field measurements of PM emission factors range from less than 0.1% to 2.2% dry matter. The larger values are mostly associated with heading fires at higher moisture contents (15 to 20% wet basis, Goss and Miller, 1973). Field estimates of PM emission factors for purely backing fires typically remain below 1%. The emission factor for particulate matter from rice straw published in the AP42 guidelines by the USEPA (1995) originates from burning tower simulations of Darley (1977; 1979). At 0.4%, the AP42 value is similar to the mean value obtained from wind tunnel studies. There is substantial variability in PM emission factor, however, depending on both the burning conditions and the quality of straw. At the time of initial design, straw samples had not been harvested and composition was unknown, so the average wind tunnel PM emission factor was therefore used to obtain estimates of the design straw consumption rate.

Rice stems meeting the CARB/industry stipulations were collected from a commercial M-202 rice crop in September 1999. Thirty stems selected at random yielded a stem weight of 2.1 ± 0.3 g dry basis (COV = 13%) with stem length of 0.86 ± 0.03 m (COV = 8%). On the basis of a mean PM emission factor of 0.35% and a chamber inlet flow rate of 230 L s^{-1} , design straw consumption rates to produce the necessary particle concentrations in the exposure chamber were estimated at 0.8 and 2.4 g min^{-1} for $200 \mu\text{g m}^{-3}$ and $600 \mu\text{g m}^{-3}$, respectively.

Of concern in meeting the design PM concentrations was the consequent concentration of CO in the chamber. Wind tunnel results yield a CO emission factor for rice straw of $4 \pm 0.9\%$ dry matter (COV = 33%; Jenkins and Turn, 1994; Jenkins, 1996). For the estimated burning rates, CO concentrations in the

³ Uncertainty is 95% confidence interval. COV = coefficient of variation = $100(\text{standard deviation}/\text{mean})$.

chamber would be in the range of 2 to 6 ppm. These concentrations are well below the OSHA 8 hour permissible exposure limit of 50 ppm, the NIOSH 8 hour recommended exposure limit of 40 ppm, and the ACGIH 8 hour threshold limit value of 25 ppm.⁴ The concentrations of CO₂ (wind tunnel emission factor of 110 ± 21% dry matter, COV = 16%) at these rates would also be well below maximum permissible exposure limits (5000 ppm).

Sufficient upstream residence time is required for equilibrium partitioning of PAH between the gas and particle phases. Previous wind tunnel studies have shown that gas-particle PAH equilibrium exists for cereal straw burning with 3 to 5 s residence time at temperatures within 20 K of ambient (Jenkins, et al., 1996b). For the purposes of maintaining temperature at the exposure chamber within typical limits, temperature of the inlet flow due to the straw burner could not increase more than 10 K without exceeding the cooling capacity of the air conditioning equipment. At the higher PM concentration and with a net straw heating value of 15 kJ g⁻¹, the burning of straw would be sufficient to raise the inlet flow temperature by 2 K. Heat loss in the system would reduce this temperature rise, but this estimate does not include the effect of any ignition system.

Cereal straw fires in the field are generally well ventilated with wind speeds in the range of 1 to 3 m s⁻¹ at 1 m height. In wind tunnel simulations at similar wind speeds and with the fire allowed to propagate naturally into the upwind fuel bed, mass air-fuel ratios ranged between 200 and 1,200 depending on the extent to which the approaching air flow was allowed to diverge immediately upstream of the fire line. Such conditions produced good matching in fire speed and flame characteristic between wind tunnel and field for different field conditions (Jenkins, et al., 1993).

Final Design

The final design of the rice straw smoke generation system consists of a straw burner and surge vessel integrated into the existing air handling system of the exposure chamber as shown in Figure 1. Purified and conditioned air is supplied from the chamber inlet duct to the straw burner. The burner is otherwise sealed against air contamination from the laboratory. Smoke exits the burner into a continuously mixed surge vessel. The surge vessel has two outlets, one (designated sample return) supplying smoke to the chamber and connecting to the main clean air duct downstream of the burner air inlet, and the second connecting via a bypass duct to the chamber exhaust. Flow rates are controlled by dampers on the outlet ducts. Smoke concentration in the chamber is controlled by regulating the fraction of flow bypassing the chamber and by controlling the straw firing interval in the burner.

⁴ Occupational Safety and Health Administration (OSHA), National Institute for Occupational Safety and Health (NIOSH), and American Conference of Governmental Industrial Hygienists (ACGIH).

The straw burner employs a shuttling system to burn singulated pre-loaded straws at a variable rate under programmable automatic control. The burner design is schematically illustrated in Figure 2. Individual stems are pre-loaded into carriers or shuttles that are in turn loaded into a magazine of vertical storage racks. Each shuttle consists of a 16 mm thick x 30 mm diameter circular brass base to which a 100 mm long by 6 mm diameter stainless steel tube is affixed. A straw is inserted into the tube and held in place by a wire spring. The main portion of the straw freely extends beyond the end of the shuttle tube. The racks are steel C-section channels with a central opening on one side allowing the straw support tubes to project from the bases that are constrained by the channel. At the lower end of each vertical rack are two solenoid-operated latches that hold and release individual shuttles under command of the electronic controller. Shuttles are released individually from each rack at any desired time interval set by the operator. A shuttle leaving a rack follows an inclined race to a central rail that turns the shuttle and the stem it carries from a horizontal to a mostly vertical, downwards hanging orientation and delivers the stem into the ignition system. The magazine with loaded shuttles is shown in Figure 3.

The ignition system consists of two identical semi-cylindrical electric furnaces facing each other across a clear span of 50 mm. The shuttle carries the straw into the space between the two furnaces and is stopped there by another solenoid-operated latch. The exposed portion of the straw hangs into the furnace where it is heated to ignition. Thermal radiation loads generated by the furnaces are similar to field conditions (irradiance of 65 kW m^{-2}). At the end of the cycle time interval, the burner controller unlatches the stop solenoid, allowing the shuttle to slide off the rail into a holding bin. The controller then cycles the rack solenoids, releasing another shuttle and straw to the furnace. Proximity switches are used to detect proper functioning of the feed system, and to signal the controller in the event of a failure. The burned portion of the stem normally breaks from the shuttle as it leaves the furnace, and freely smolders until spent. With longer cycle time intervals, smoldering is usually complete before the controller unlatches the shuttle. The portion of stem inside the shuttle tube usually remains unburned, and in this way simulates the unburned stubble in the field. The furnaces can be seen below the straw magazine in Figures 2 and 3, and in operation in Figure 4.

The straw magazine and furnaces are situated inside the sealed burner. The burner shell is constructed of stainless steel except for the front door that is of clear polycarbonate so that the function of the burner can be observed while in operation. A radiation shield is placed between the furnaces and the door to reduce heating of the plastic. The burner also includes sensors and actuators for automatic fire suppression if needed.

The burner inlet air flow rate was specified from a mass air-fuel ratio of 1,200 and a fuel burning rate of 2.4 g min^{-1} at the higher particle concentration. The air-fuel

ratio was selected to match the highest value employed in wind tunnel studies, and to insure adequate air for off-design operation if desired. This air-fuel ratio requires a burner flow of 40 L s^{-1} , representing less than 20% of the total conditioned air flow (230 L s^{-1}) available upstream of the burner inlet.

The burner produces a periodic variation in concentration in its outlet flow due to the use of a discrete firing interval to burn the straw. In order to decrease the peak concentration and broaden the distribution over the burning cycle, a 1 m^3 fan-mixed surge vessel was installed between the burner and the exposure chamber. The surge also helps to cool the burner flow before it joins the main airflow to the chamber. Under continuous operation the furnaces generate a total heat output of 4.8 kW. When firing at the shorter time interval to produce a higher particle concentration, the heat release from straw burning is approximately 0.6 kW, yielding a total burner heat output of 5.4 kW that is sufficient to raise the outlet gas temperature by 112 K. If all burner flow were mixed back into the main inlet flow, the overall temperature rise at the chamber (neglecting duct heat losses) would be about 20 K. Additional heat transfer surface was desired to reduce the temperature rise in the chamber flow so as to stay within the control range of the existing air handling system. Potential particle losses to the surfaces were considered to be less serious than the inability to control temperature or to produce a more uniform particle concentration at the chamber. Particle losses to the walls have not so far been a problem.

System Performance and Smoke Characteristics

Fuel consumption and burning times

Burning and emission characteristics were investigated using hand-cut ground-level harvested straw satisfying CARB stipulations as described above. The fraction of stem burned averaged 78% of that loaded, the rest remaining mostly unburned in the shuttle support tube. Of the portion of the stem burned, 17% remained as ash.

Burning of a straw typically occurs in three stages: 1) induction, 2) flaming combustion, and 3) glowing combustion and smoldering. After arriving in the furnace, the straw undergoes heating and begins to pyrolyze, releasing smoke particles and volatiles that ignite in a luminous flame. In practice the straw sometimes does not ignite all at once, but instead several separate ignitions may occur along the stem. After flaming stops, residual char burns in a glowing combustion and the straw smolders for some time. Smoke is emitted throughout all three stages. Occasionally the volatiles fail to ignite a flame, but long-term observations indicate this occurs less than 10% of the time. The induction period usually lasts about 3 s prior to ignition, flaming lasts about 4 s, and smoldering is visible for roughly 10 s following extinction of the flame although some emission probably continues beyond this. The particle emission factor, particle size

distribution, and chemical composition are likely related to the duration of these periods, but the effects have not yet been fully investigated.

Intermittency in burning and chamber concentrations

The periodic behavior of the burner is evident in the CO₂ concentrations measured at the burner exit shown in Figure 5. These results were obtained with a firing interval of 30 s. CO₂ was measured using a non-dispersive infrared (NDIR) analyzer (Model AR-60, Anarad, Inc., Santa Barbara, California). Sampling at the burner exit is shown for the first 10.5 min in Figure 5. There is some lag in the gas sampling system, but the large variation in concentration is apparent. There is also a variation in peak CO₂ concentration due to differences in individual straw weights and burning characteristics, although emission profiles remain similar. For the period shown, peak CO₂ concentration is $1,716 \pm 312$ ppmv with a COV of 40% (background CO₂ concentration of 350 ppmv). Variation in the burner outlet gas temperature, also shown in Figure 5, is similarly due to the periodic straw burning. During the period shown, four ignition failures occur, representing a 19% failure rate. This is somewhat higher than occurs under normal testing, and is due in part to the furnaces being set at a lower temperature (400°C as measured by a thermocouple in the space between the furnaces) before the standard operating temperature (450°C) was established, and the furnaces not being fully warmed up prior to starting the test. For these tests, the burner air flow rate of 50 L s⁻¹ was also 25% higher than normal, thereby reducing the heating rate of the fuel in the furnace.

The impact of the surge on dampening peak CO₂ fluctuations and generating a more uniform concentration is also evident in Figure 5. After 10.5 min, the gas sampling inlet was moved to the surge outlet. The figure shows the impacts of mixing the surge volume on both concentration and temperature. With the fan off (between 20.5 and 25 min in Figure 5), peak CO₂ concentration increases, as does outlet gas temperature, both indicating short-circuiting of the flow from inlet to outlet. Gas temperature declines 25 to 30 K due to heat loss in the surge.

Flow rates and firing intervals

Flow rates were measured in the burner inlet duct, sample return flow duct, and bypass duct. Burner inlet flow was set at the design flow rate of 40 L s⁻¹. To yield the desired particle concentrations in the chamber (see below), flow from the surge to the chamber inlet air supply duct was set at 11 L s⁻¹, or 28% of burner flow, with 29 L s⁻¹ diverted through the bypass.

Total PM concentrations were measured gravimetrically on 30 min filter samples collected from the exposure chamber. In making these measurements, the sample inlet position was fixed near the inhalation point of a subject sitting at rest in the chamber. The chamber was not traversed, thus PM concentrations do not necessarily represent mean values for the chamber. This sample inlet position

was used for all sampling from the chamber, including particle size distribution measurements described later. From preliminary measurements of PM concentration, the firing interval for the burner was set at 45 s for the high concentration, and 140 s for the low concentration, keeping the sample return flow fixed.

Air-fuel ratio

The overall burner mass air-fuel ratios are 2,140 at the 45 s firing interval (high concentration) and 6,660 at the 140 s firing interval (low concentration). These are well in excess of the minimum design value of 1,200. Not all of the burner inlet air flows through the furnace slot, as some can enter the smoke hood over the top of the furnaces. Actual air-fuel ratio at the straw has not been directly measured and is less than the overall value, but air supply appears to be adequate.

Residence times

Duct dimensions and volumes were shown in Figure 1. For the final flow rates selected, the smoke residence time prior to reaching the exposure chamber is 35 s. Of this, 25 s is associated with the surge, and 3 s is spent in the diluted flow upstream of the chamber. The temperature of the diluted flow is within 2 K of the conditioned air temperature ahead of the burner due to heat loss in the surge and mixing with the cold main flow. Total residence time, including the exposure chamber volume, is 117 s. Gas velocities are sufficiently high to generate turbulent flow (duct Reynolds numbers between 6×10^3 and 5×10^4) and well-mixed conditions in the ducts.

Particle concentrations

Actual chamber particle concentrations from 13 low level exposures and 10 high level exposures are listed in Table 2. Also listed in the table are results from five low-concentration same-subject serial day exposures (exposures conducted on successive days). Individual exposures at low concentration were conducted over a period of 7 months, individual high concentration exposures were conducted over 5 months, and serial day exposures were conducted over 4 months. Most exposures lasted 30 min. The measured concentrations are 6 to 21% lower than the target concentrations. For all three series, the 95% confidence intervals are 23 to 28% of the mean concentration, although the COV for the serial day exposure is half the individual exposures.

Particle emission factors

PM emission factors were derived from the measured PM concentrations, gas flow rates, and dry straw consumption rates. The low concentration of $188 \pm 45 \mu\text{g m}^{-3}$ gives an estimated emission factor of $1.89 \pm 0.45\%$ dry matter. The high

concentration of $508 \pm 144 \mu\text{g m}^{-3}$ yields $1.65 \pm 0.47\%$ dry matter. The serial day exposure concentration of $158 \pm 40 \mu\text{g m}^{-3}$ yields an emission factor of $1.59 \pm 0.40\%$ dry matter. The differences are not significant at the 95% confidence level. The aggregate PM emission factor for all three categories is $1.75 \pm 0.25\%$ dry matter (COV = 37%). These emission factors are 4 to 5 times higher than the mean value of 0.35% assumed from the average of all wind tunnel studies, and about 2.5 times the peak value resulting from the wind tunnel studies conducted on rice straw of similar moisture content. Wind tunnel PM emission factors are correlated with straw composition, and in particular, the amount of potassium in the straw (Jenkins, 1996). Regression of wind tunnel PM against K concentration (% dry matter) yields $\text{PM (\% dry matter)} = 0.21(\text{K}) + 0.05$ ($r^2 = 0.904$). For the type 1 straw used in the exposure experiments, the 2.35% K concentration gives a predicted PM emission factor of 0.54%, 50% higher than the average wind tunnel result, but still about 3 times lower than the average burner value of 1.75%. PM emission is also related but not as strongly correlated to Cl concentration ($\text{PM} = 0.41(\text{Cl}) + 0.20$; $r^2 = 0.355$). Mechanisms yielding higher PM emission factors due to higher K concentrations are not specifically identified, but the catalytic effects of alkali, coupled with higher emissions of KCl crystals (routinely observed with filter samples of rice straw smoke) could be involved.

A number of factors potentially contribute to the differences in emission factor, including non-uniform concentration in the exposure chamber. The estimates of emission factor assume complete mixing in the chamber. Other factors include errors in the PM concentration, air flow, and straw consumption rate measurements. The smoke release during the induction period before flaming begins may also contribute to higher PM concentrations. In the field and wind tunnel backing fires, volatiles emitted during heating are more likely to ignite and burn in flaming combustion, hence particle emission rate may be reduced in such continuous fires. Backing fires are thought to generate lower PM emissions in comparison with heading fires through this mechanism (Goss and Miller, 1973). Wind tunnel measurements were made only in backing fires (Jenkins, 1996). Strip-light fires do not exhibit purely backing behavior, and may generate higher PM emission factors, although the wind tunnel experiments show that pure backing fires can also produce high emission factors under some conditions. Ignition failures in the burner may also disproportionately influence particle emission factors, but the failure rates in the exposure experiments are well below 10%. Potential errors involved in the burner measurements are generally smaller than those associated with either field or wind tunnel measurements, and so the burner emission factors may be more accurate. In any case, the emission factors are higher than design values. Particle concentrations, rather than emission factors, serve as the basis for the burner control. PM concentrations are repeatable and maintained close to target concentrations. Further characterization of particle properties is needed to determine if the higher emission factors are indicative of qualitative differences in the smoke that would constitute difficulties in interpretation of the exposure results.

Transient performance and predictions of the surge and chamber concentrations

The effect of the surge volume on the peak CO₂ concentration was noted above. The concentration at the surge outlet is not uniform over time, but the variability has been substantially reduced in comparison with the burner outlet. The concentration at the surge outlet was predicted from the burner outlet by means of a transient mass balance assuming well-mixed conditions (equation [1]).

$$\frac{dC_s}{dt} = \frac{\dot{V}_{st} T_s}{V_s T_{st}} [C_b - C_s] \quad [1]$$

C_s = concentration in surge

C_b = concentration in burner outlet flow

t = time (s)

\dot{V}_{st} = flow rate into surge at standard conditions (m³ s⁻¹)

V_s = surge volume (m³)

T_s = surge temperature (K)

T_{st} = standard temperature (K)

The resulting differential equation was integrated numerically using a simple Euler technique. A similar analysis was performed for the exposure chamber, again assuming well-mixed conditions. The predicted concentration in the chamber was estimated from a numerically integrated transient mass balance (equation 2).

$$\frac{dC_c}{dt} = \frac{1}{V_c} \frac{T_c}{T_{st}} [\dot{V}_{st,s} (C_s - C_c) + \dot{V}_{st,o} (C_o - C_c)] \quad [2]$$

C_c = concentration in chamber

t = time (s)

V_c = chamber volume (m³)

T_c = chamber temperature (K)

$\dot{V}_{st,s}$ = flow rate from surge to chamber at standard conditions ($\text{m}^3 \text{s}^{-1}$)

$\dot{V}_{st,o}$ = flow rate of air mixing with surge sample return at standard conditions ($\text{m}^3 \text{s}^{-1}$)

C_s = concentration in surge flow

C_o = concentration in air mixing with surge flow

Predicted surge and chamber concentrations are shown in Figure 6. The profiles are derived from the actual CO_2 concentration profile measured at the burner outlet over a single straw firing cycle of 1 min that is also shown in the figure. The concentration at the burner outlet peaks above 2,500 ppm, with a duration of approximately 10 s in the primary peak region. Smoldering continues for some time past the visible limit as evidenced by the continuing decline in concentration. Also shown in the figure are the gas temperatures at the burner and surge outlets. The lag in the CO_2 sampling system is evident in the displacement of the concentration peak by 4 s relative to that of temperature (no attempt has been made to shift the concentration profile by correcting for the lag time).

The surge outlet concentration profile predicted from the burner measurements shows a peak concentration around 800 ppm, similar to the data of Figure 5 as noted above. For comparison, an actual profile measured at the surge outlet is also shown in Figure 6. Unfortunately, burner and surge concentrations could not be measured simultaneously, so the actual surge outlet profile is only representative of the profile predicted from the burner profile shown. The predicted and actual surge outlet concentration profiles are, however, quite similar. The predicted concentration profile in the chamber is also shown in the figure.

As described above, an important element of testing was to be able to bring the chamber up to the target concentration quickly. The transient response of the chamber is predicted by equations [1] and [2]. To provide estimates of the transient particle concentrations, the fractional particle mass release profile was assumed to be identical to that for the fractional CO_2 release. Instantaneous particle concentration profiles could not be obtained and only integrated particle concentrations were obtained from the filters. From the CO_2 concentration measured at the burner outlet (and shown in Figure 6), the mass conversion fraction and cumulative mass conversion were obtained as shown in Figure 7. Both curves bear good resemblance to results obtained via thermogravimetric analysis (TGA) of rice straw, and show the characteristic pyrolysis and char oxidation regimes (Bining and Jenkins, 1992). The cumulative conversion implies a much longer smoldering time than visual observation suggests.

Transient particle concentrations predicted from the above assumptions are shown in Figures 8 and 9 for the two firing intervals of 45 and 140 s. These predictions are based on the particle emission factors for the low and high concentrations obtained from filter samples as described above.

For the high concentration exposures with a firing interval of 45 s, the chamber achieves its equilibrium concentration within 6 cycles, or 4.5 min. Concentration fluctuates over a range of $50 \mu\text{g m}^{-3}$ between roughly 475 and $525 \mu\text{g m}^{-3}$ within firing cycles under these assumptions. For the 140 s interval, the concentration profile becomes steady after 2 cycles, or about 4.7 min. The fluctuation in chamber concentration is larger, ranging $150 \mu\text{g m}^{-3}$ between 100 and $250 \mu\text{g m}^{-3}$. Although the chamber concentration fluctuates due to the periodic firing of straws, in each case the mean target concentration is achieved within 5 min.

As a surrogate to transient particle concentration, transient CO concentration was determined and compared against predicted values for both firing intervals. Results are shown in Figure 10. Experimental and predicted behaviors are in good correspondence for predictions based on a CO emission factor of 5% dry matter, a value 25% greater than the average wind tunnel value of 4%. The experimental results reveal the natural variability occurring due to differences in stem mass, ignition quality, and burning characteristics among straws. Times to bring the chamber up to target concentration are matched to the predictions made under the assumption of well-mixed conditions.

Particle size distributions were obtained using a scanning mobility particle sizer (SMPS) employing a differential scanning mobility analyzer with condensation nuclei counter to obtain size distributions in the range up to 1000 nm. Samples were drawn from the same location as the total filters. For these tests, sampling flow rates were set to yield distributions over the range of 20 to 930 nm, with total scanning time per sample of 75 s. The relatively long scanning time for the SMPS leads to some difficulty in interpreting the size distributions for the longer firing intervals due to the larger fluctuation in concentration over the cycle. The shorter 45 s firing interval was used to generate a more steady concentration of particles in the chamber during these measurements. Scans were run during the period immediately following burner start, during steady operation, and during the smoke clearing period after stopping the burner. Number distributions are shown in Figure 11 along with mass concentrations and mass mean diameters (MMD) determined from the SMPS results. In the period between 2.5 min and 6 min following burner start, peak particle size decreased from 100 nm to 55 nm, implying some loss of fine particles to the walls of the system. Size distribution was steady after 6 min, as were concentrations. MMD decreased 20% while mass concentration increased from 186 to $600 \mu\text{g m}^{-3}$. Clearing of particles from the chamber was fairly rapid.

Cumulative particle size distributions for the chamber obtained from the SMPS (20-930 nm) were compared with earlier wind tunnel distributions (380 nm – 10

µm) obtained by cascade impactor. As shown in Figure 12, alignment of the cumulative distributions shows the fraction in the range below 930 nm to account for approximately 80% of mass.

Average concentrations and firing intervals

For the purposes of experimental design, mean concentrations as functions of emission factor and firing interval are given in Figures 13-15 for particulate matter, CO, and CO₂. Concentrations of CO and CO₂ do not exceed recommended limits for any of the likely conditions obtained under actual testing with rice straw and similar fuels. As noted above, CO measurements yield a 5% emission factor that is in good agreement with emission factors from wind tunnel and field testing.

Summary and Conclusions

A unique smoke generation system was designed for the purposes of exposing human subjects to smoke from rice straw burning under highly controlled conditions. The system burns individual stems or stem sections to produce particle concentrations up to 900 µg m⁻³ in a temperature and humidity controlled exposure chamber. Higher concentrations are possible but have not so far been tested. Burner operation is fully automatic and programmable. Straw ignition is performed under radiant heating from electric furnaces, and simulates ignition from flame radiation in the field. Particle concentration is controlled by varying the time interval between ignitions, and by changing the ratio of burner outlet flow mixing with the main purified air supplied to the exposure chamber. A well-mixed surge volume between the burner and the chamber sample return duct produces a more uniform concentration at the exposure chamber. The system achieves steady-state chamber particle concentrations within 5 minutes from initial firing. Repeatability of particle concentration is excellent for test concentrations of 200 and 500 µg m⁻³ and experiments ranging over 5 months.

Particle concentrations are controlled to good precision, but estimated particle emission factors are higher than previously obtained from field and wind tunnel studies. Wind tunnel simulations yield total particulate matter (PM) emission factors ranging from 0.063 to 0.86% dry matter for rice straw with a global average of 0.35%. Field studies of rice straw burning yield PM emission factors ranging from <0.1% to 2.2%, but generally between 0.3 and 1% for pure backing (wind opposed) fires. The range in actual field emission factors for the types of fires permitted by regulation in California (heading fires are excluded) is not entirely known. From potassium concentration in the straw used (2.35% dry matter), wind tunnel derived correlations predict a PM emission factor of 0.54%. PM emission factors from the rice straw smoke generation system range from 1.2 to 2.3% dry matter with an overall average of 1.75%. These emission factors are 4 to 5 times higher than the mean value of 0.35% assumed for design purposes,

and average about 3 times the value resulting from wind tunnel studies conducted on straw of similar composition and moisture. A number of factors can contribute to the differences, but of particular interest are smoke emissions during the heating period before flaming begins and the occasional ignition failures that occur in the burner. These constitute the primary deviations from smoke emission in pure backing fires used for comparison. Particle size distributions are similar to field and wind tunnel measurements, with 80% of mass or more below 1 μm , but particle properties need further characterization to examine possible compositional differences between chamber and actual environmental smoke exposures.

References

Bining, A.S. and Jenkins, B.M. (1992). Thermochemical reaction kinetics for rice straw from an approximate integral technique. ASAE Paper No. 926029, American Society of Agricultural Engineers, St. Joseph, MI.

Darley, E.F. (1977). Emission factors from burning agricultural wastes collected in California. Final Report, CARB Project 4-011, California Air Resources Board, Sacramento, California.

Darley, E.F. (1979). Hydrocarbon characterization of agricultural waste burning. Final Report, CARB Project A7-068-30, California Air Resources Board, Sacramento, California.

Goss, J.R. and Miller, G.E. Jr. (1973). Study of abatement methods and meteorological conditions for optimum dispersion of particulates from field burning of rice straw. Final Report, CARB Project 1-101-1, California Air Resources Board, Sacramento, California.

Jacobs, J., Kreutzer, R. and Smith, D. (1997). Rice burning and asthma hospitalizations, Butte County, California, 1983-1992. *Environ. Health Perspect.* 105(9):980-985.

Jenkins, B.M., Turn, S.Q. and Williams, R.B. (1992). Atmospheric emissions from agricultural burning in California: determination of burn fractions, distribution factors, and crop specific contributions. *Agriculture, Ecosystems, and Environment* 38:313-330.

Jenkins, B.M., Kennedy, I.M., Chang, D.P.Y, Raabe, O.G., Turn, S.Q., Williams, R.B., Hall, S.G. and Teague, S. (1993a). Sensitivity of flame structure and particulate matter emissions to the operating configuration of a combustion wind tunnel. Final Report, Project No. A932-161, California Air Resources Board, Sacramento, California.

Jenkins, B.M., Kennedy, I.M., Turn, S.Q., Williams, R.B., Hall, S.G., Chang, D.P.Y, Raabe, O.G. and Teague, S.V. (1993b). Wind tunnel modeling of atmospheric emissions from agricultural burning: influence of operating configuration on flame structure and particle emission factor for a spreading type fire. *Environmental Science and Technology* 27(9):1763-1775.

Jenkins, B.M. and Turn, S.Q. (1994). Primary atmospheric pollutants from agricultural burning: emission rate determinations from wind tunnel simulations. ASAE Paper 946008, ASAE, St. Joseph, Michigan.

Jenkins, B.M., Jones, A.D., Turn, S.Q. and Williams, R.B. (1996a). Emission factors for polycyclic aromatic hydrocarbons (PAH) from biomass burning. *Environmental Science and Technology* 30(8):2462-2469.

Jenkins, B.M., Jones, A.D., Turn, S.Q. and Williams, R.B. (1996b). Particle concentrations, gas-particle partitioning, and species intercorrelations for polycyclic aromatic hydrocarbons (PAH) emitted during biomass burning. *Atmospheric Environment* 30(22):3825-3835.

Jenkins, B.M., Bakker, R.R. and Wei, J.B. (1996c). On the properties of washed straw, *Biomass and Bioenergy* 10(4):177-200.

Jenkins, B.M. (1996). Atmospheric pollutant emission factors from open burning of agricultural and forest biomass by wind tunnel simulations. Final Report (3 Vols.), CARB Project A932-126, California Air Resources Board, Sacramento, California.

Lawson, R.J., Schenker, M.B., McCurdy, S.A., Jenkins, B., Lischak, L.A., John, W. and Scales, D. (1995). Exposure to amorphous silica fibers and other particulate matter during rice farming operations, *Appl. Occup. Environ. Hyg.* 10(8):677-684.

Torigoe, K., Hasegawa, S., Numata, O., Yazaki, S., Matsunaga, M., Boku, N., Hiura, M. and Ino, H. (2000). Influence of emission from rice straw burning on bronchial asthma in children. *Pediatrics International* 42:143-150.

Turn, S.Q., Jenkins, B.M., Chow, J.C., Pritchett, L.C., Campbell, D., Cahill, T. and Whalen, S.A. (1997). Elemental characterization of particulate matter emitted from biomass burning: wind tunnel derived source profiles for herbaceous and wood fuels, *Journal of Geophysical Research* 102(D3):3683-3699.

USEPA. (1995). Compilation of air pollutant emission factors, AP42. US Environmental Protection Agency, Research Triangle Park, North Carolina.

Williams, P.T. and Horne, P.A. (1994). The role of metal salts in the pyrolysis of biomass. *Renewable Energy* 4(1):1-13.

Table 1. Average composition of rice straw (variety M-202) burned during exposures.

Higher Heating Value (MJ/kg dry basis)	16.27
Proximate Analysis (% dry matter)	
Ash	16.10
Volatiles *	70.17
Fixed Carbon **	13.73
Elemental Analysis (% dry matter)[†]	
C	41.95
H	4.18
N	0.69
S	0.11
Cl	0.63
Si	5.25
Al	0.02
Ti	<0.01
Fe	0.05
Ca	0.36
Mg	0.25
Na	0.19
K	2.21
P	0.17
O (by difference)	43.96
Ash Composition (% ash)	
SiO ₂	69.72
Al ₂ O ₃	0.61
TiO ₂	0.04
Fe ₂ O ₃	0.41
CaO	3.15
MgO	2.58
Na ₂ O	1.55
K ₂ O	16.55
P ₂ O ₅	2.48
SO ₃	0.88
Cl	2.98
CO ₂	0.35
Total	101.29

* mass fraction volatilized upon heating at 950°C in an oxygen free atmosphere.

** mass fraction of carbonaceous material not in ash or volatiles.

[†]Elements Si – P derived from ash composition and ash concentration.

Table 2. Chamber PM concentrations from exposure tests.

	Low Concentration	High Concentration	Serial Day Exposure*
Straw Firing Interval (s)	140	45	140
Target PM Concentration ($\mu\text{g m}^{-3}$)	200	600	200
Mean PM Concentration ($\mu\text{g m}^{-3}$)	188	508	158
Number of tests	13	10	5
Range ($\mu\text{g m}^{-3}$)	274	576	87
Minimum ($\mu\text{g m}^{-3}$)	93	310	117
Maximum ($\mu\text{g m}^{-3}$)	367	886	204
Standard deviation	75	202	32
Standard error	21	64	14
95% confidence interval ($\mu\text{g m}^{-3}$)	± 45	± 144	± 40
Coefficient of Variation (%)	40	40	20

* exposures conducted on the same subject on successive days.

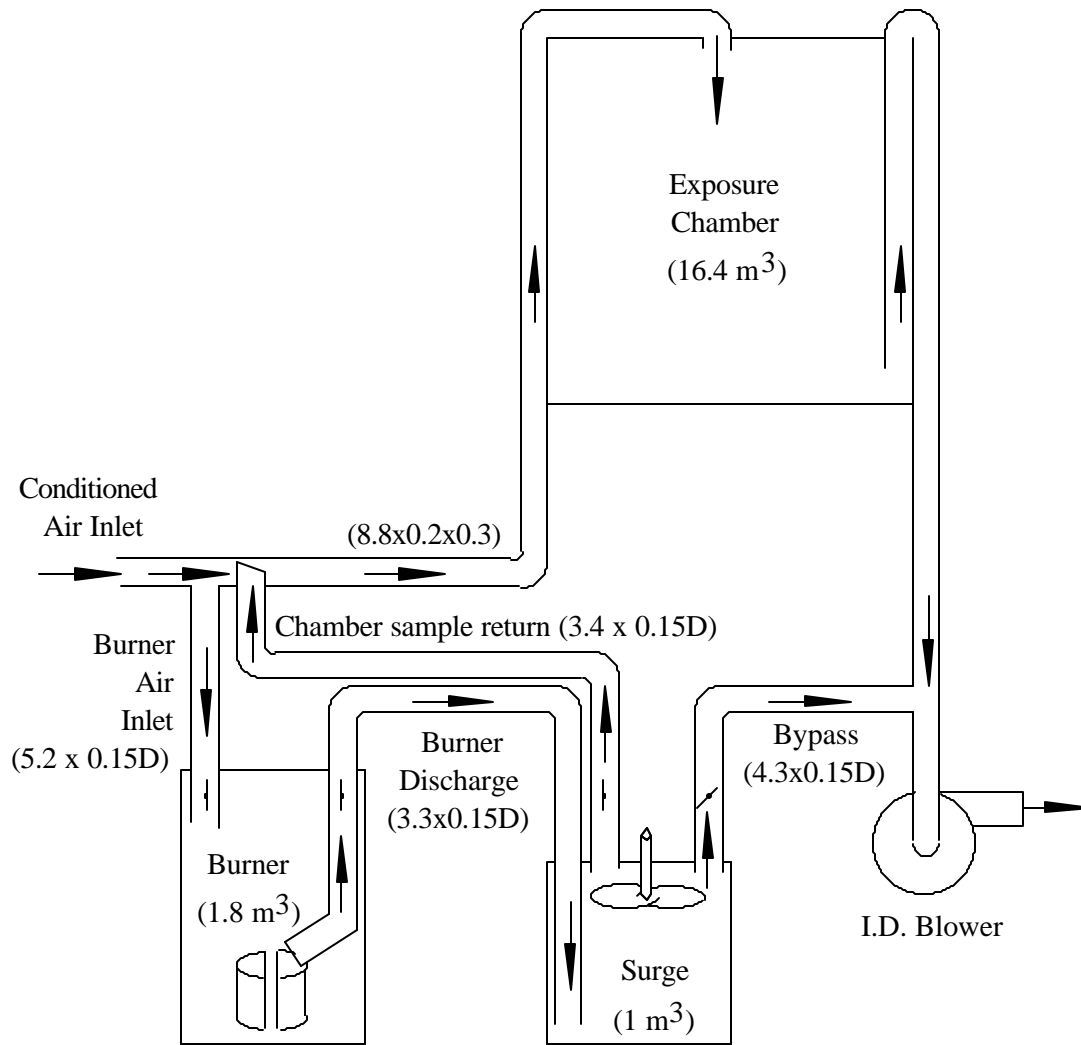


Figure 1. Smoke generation and distribution system. Duct dimensions are given as length x diameter (D) or length x rectangular cross section in meters; volumes in cubic meters.

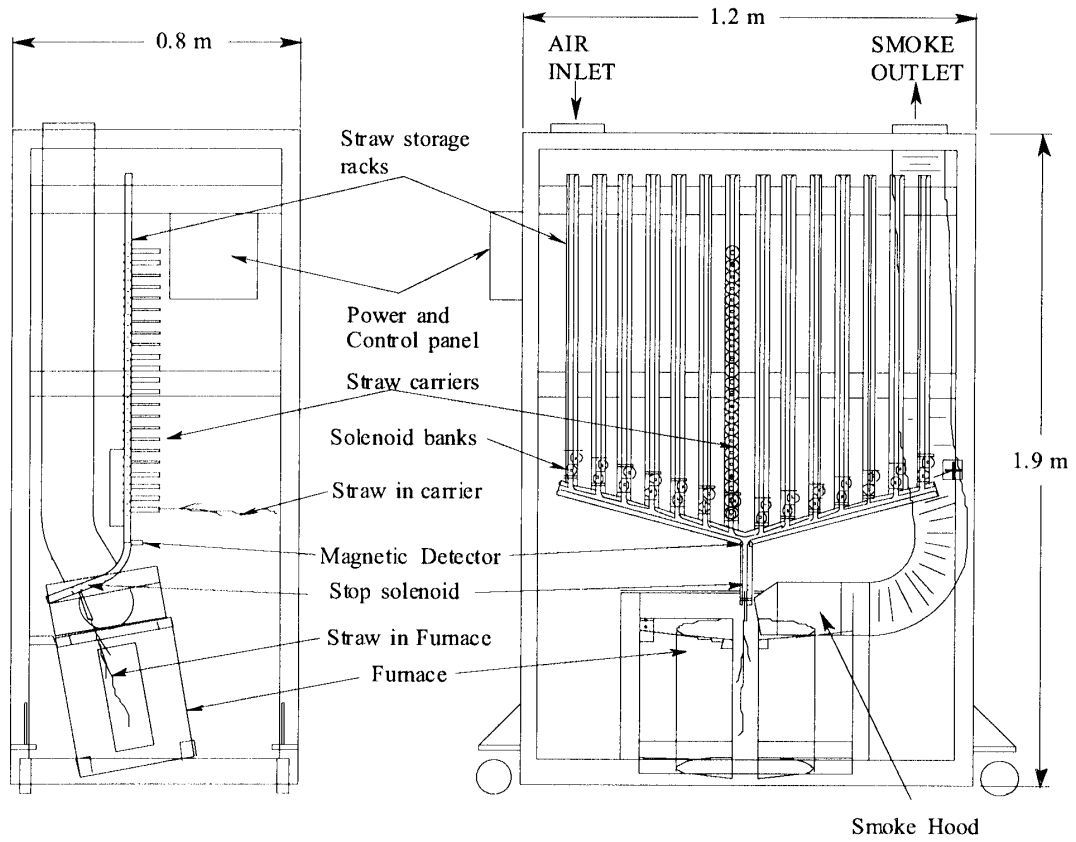


Figure 2. Schematic of the straw storage magazine and burner.

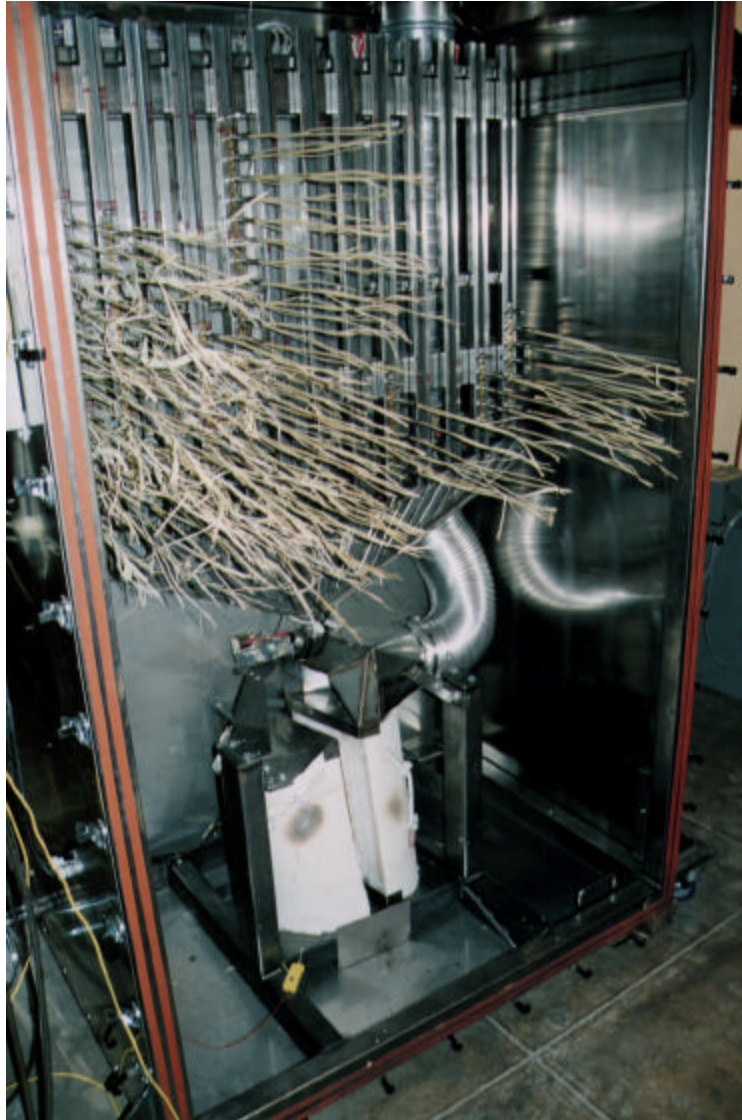


Figure 3. View of burner interior showing straw storage magazine with shuttles and pre-loaded straw. Ignition furnaces are located below the magazine. The smoke hood is situated at the top of the right furnace. The front polycarbonate door has been removed for loading.

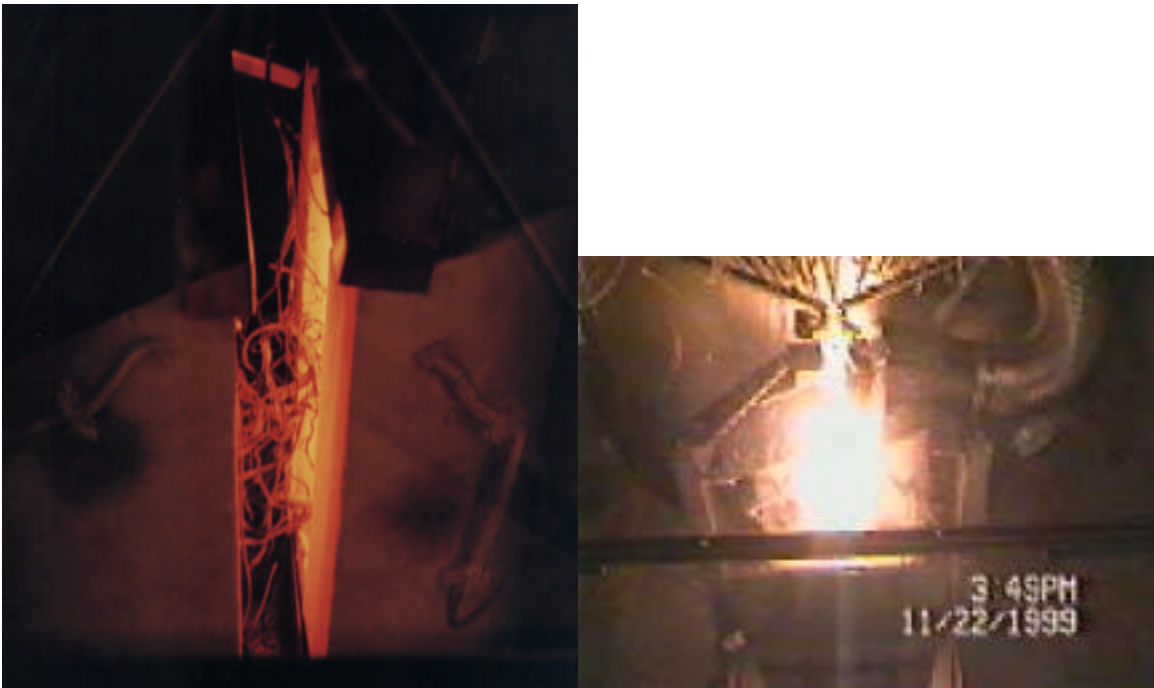


Figure 4. View of ignition furnaces during operation. Left: showing thermal radiation intensity. Right: at peak flaming after igniting a straw.

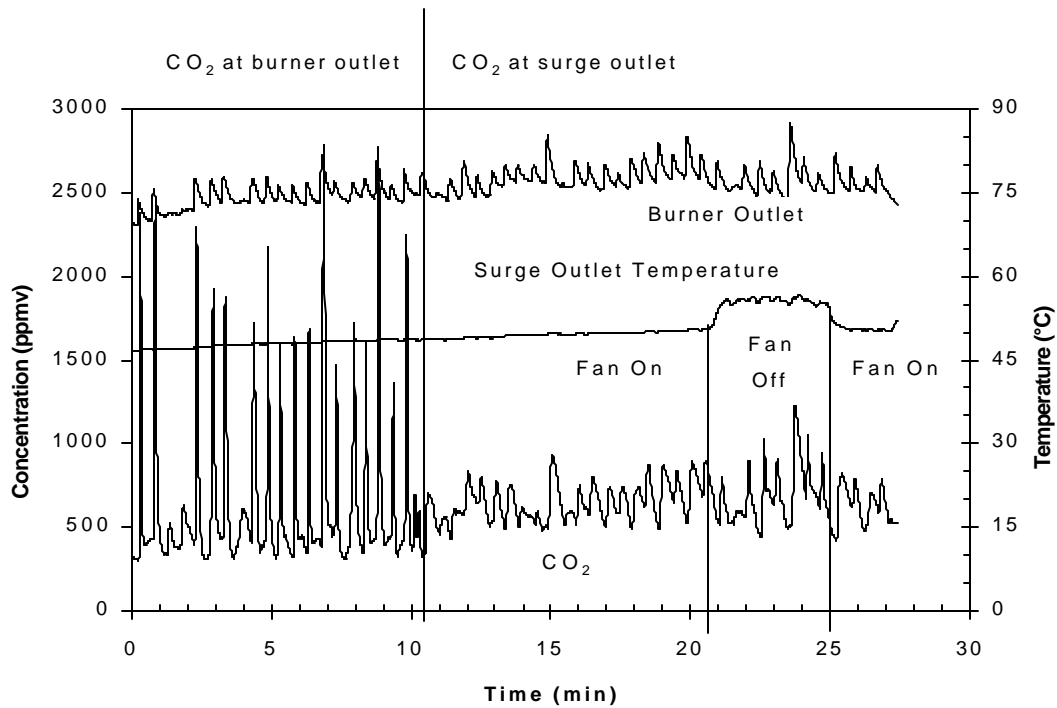


Figure 5. CO₂ concentrations and temperatures at burner and surge outlets for a 30 s firing interval with rice straw. The surge outlet temperature rise between 20 and 25 min is caused by turning off the mixing fan during this period. The gas sampling line was moved from the burner outlet to the surge outlet at 10.5 min (simultaneous sampling was not performed).

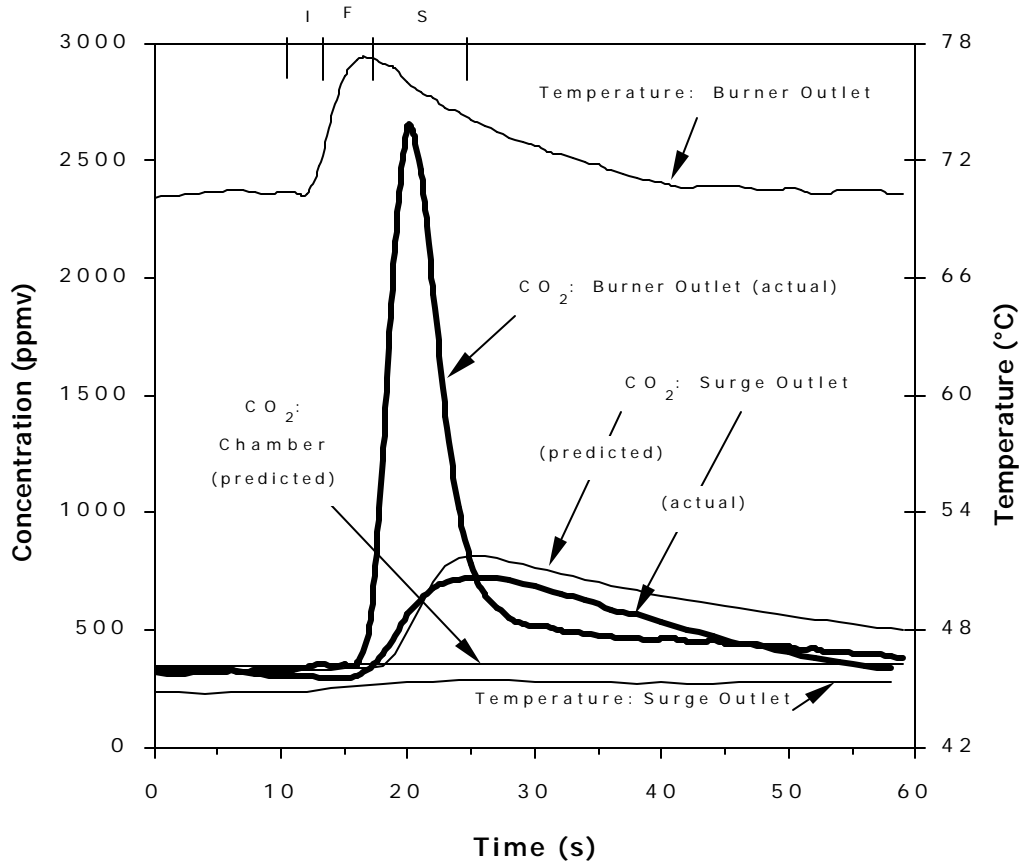


Figure 6. CO₂ concentration at the burner outlet (actual), surge outlet (actual and predicted), and exposure chamber (predicted) for a single firing cycle. Actual temperatures at the burner and surge outlets also shown. Combustion stages from visual observations shown at top and positioned relative to the temperature profile: I = induction period, F = flaming, S = glowing combustion and smoldering (smoldering period may extend beyond visible limit indicated). Actual surge outlet concentration not simultaneous with burner outlet concentration and shown for illustrative purposes. Lag in sampling system causes concentration profiles to be shifted approximately 4 s in time relative to the temperature profiles.

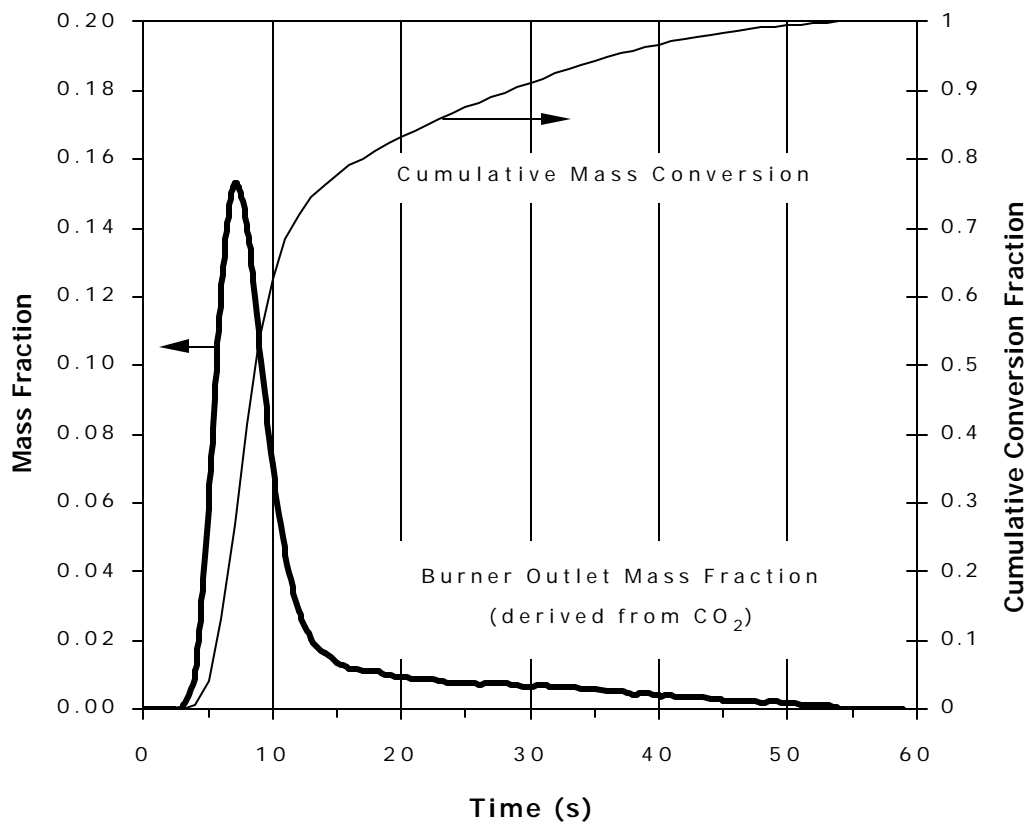


Figure 7. Straw mass conversion fraction and cumulative conversion estimated from CO₂ concentrations at burner outlet.

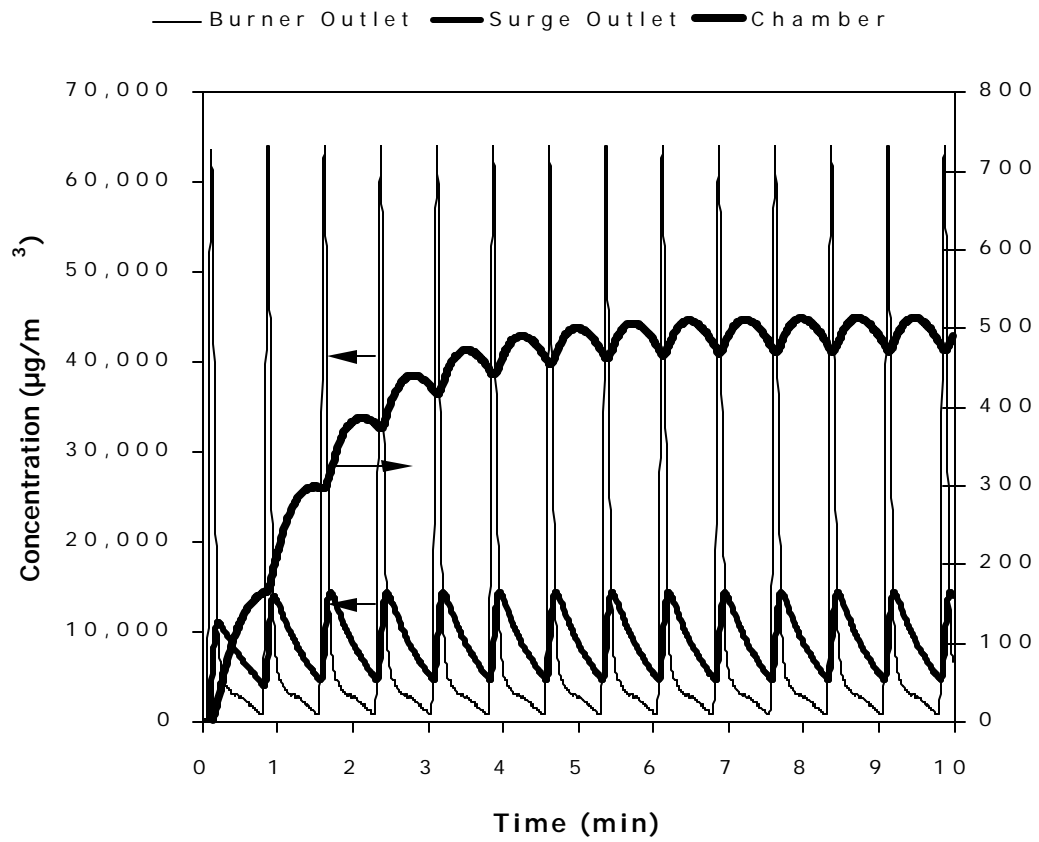


Figure 8. Predicted particle concentrations in surge and exposure chamber from estimates of transient particle concentrations at the burner outlet, 45 s firing interval.

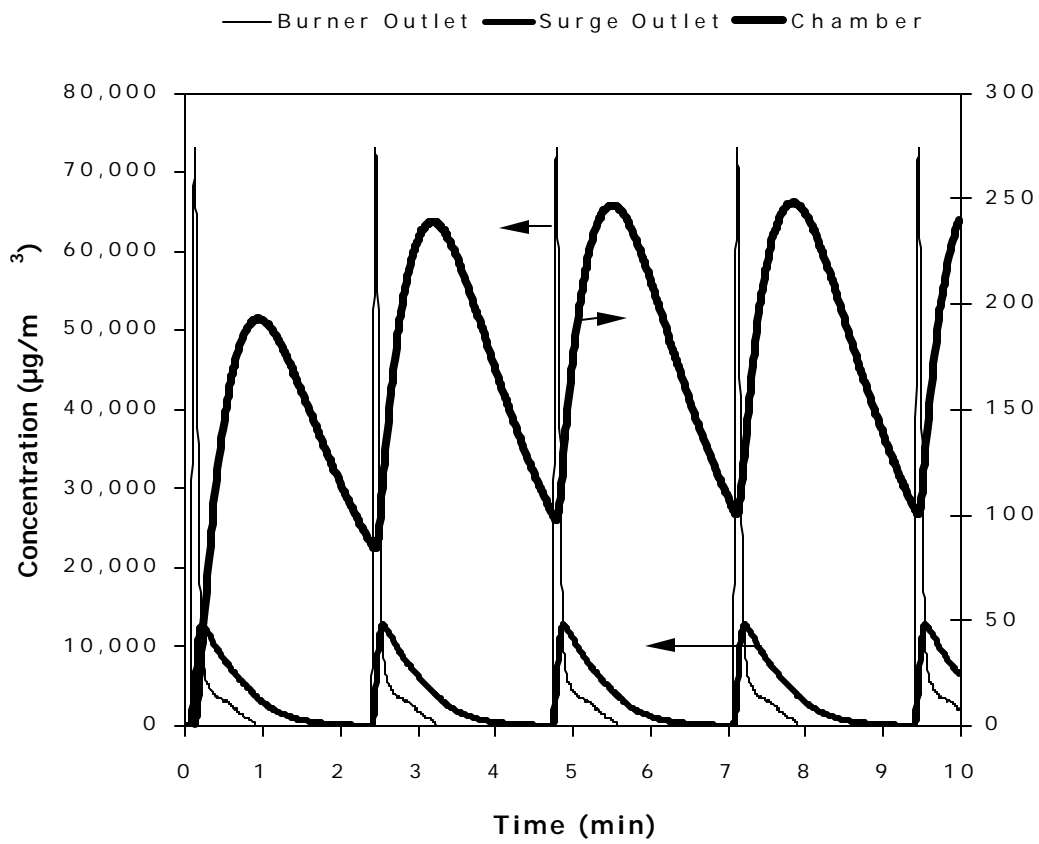


Figure 9. Predicted particle concentrations in surge and exposure chamber from estimates of transient particle concentrations at the burner outlet, 140 s firing interval.

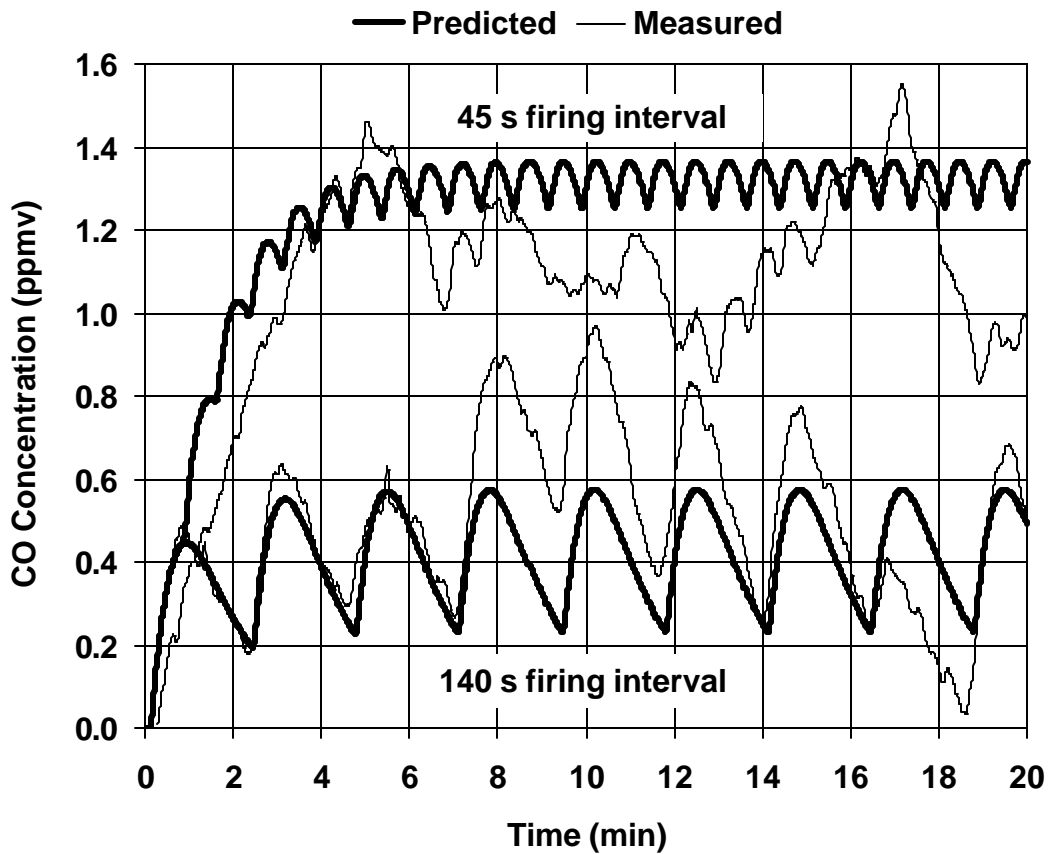


Figure 10. Predicted and measured CO concentrations (ppmv) in the exposure chamber for 45 and 140 s firing intervals. CO emission factor used for predictions = 5% dry matter.

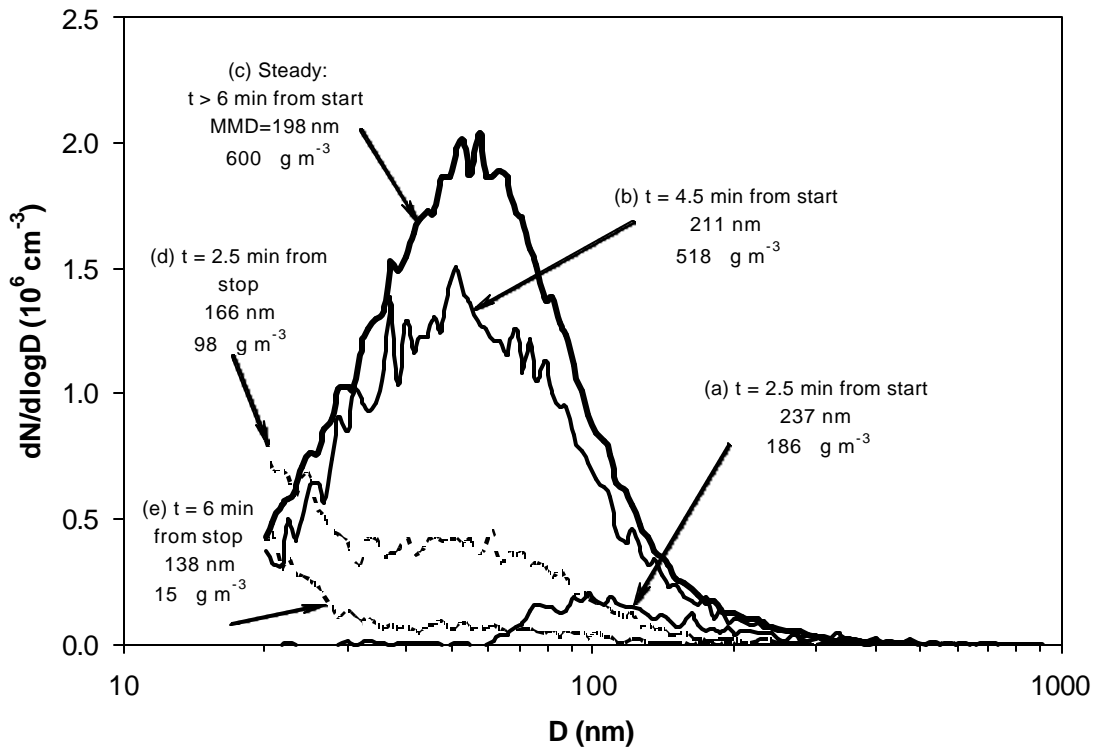


Figure 11. Particle size number distributions for smoke in the exposure chamber with a 45 s firing interval: (a) 2.5 min after starting to fire straw, (b) 4.5 min after starting, (c) steady operation after 6 min, (d) 2.5 min after stopping straw firing, and (e) 6 min after stopping. Also shown are geometric mass mean diameters and total mass concentrations as determined by SMPS for the size interval 20 to 930 nm.

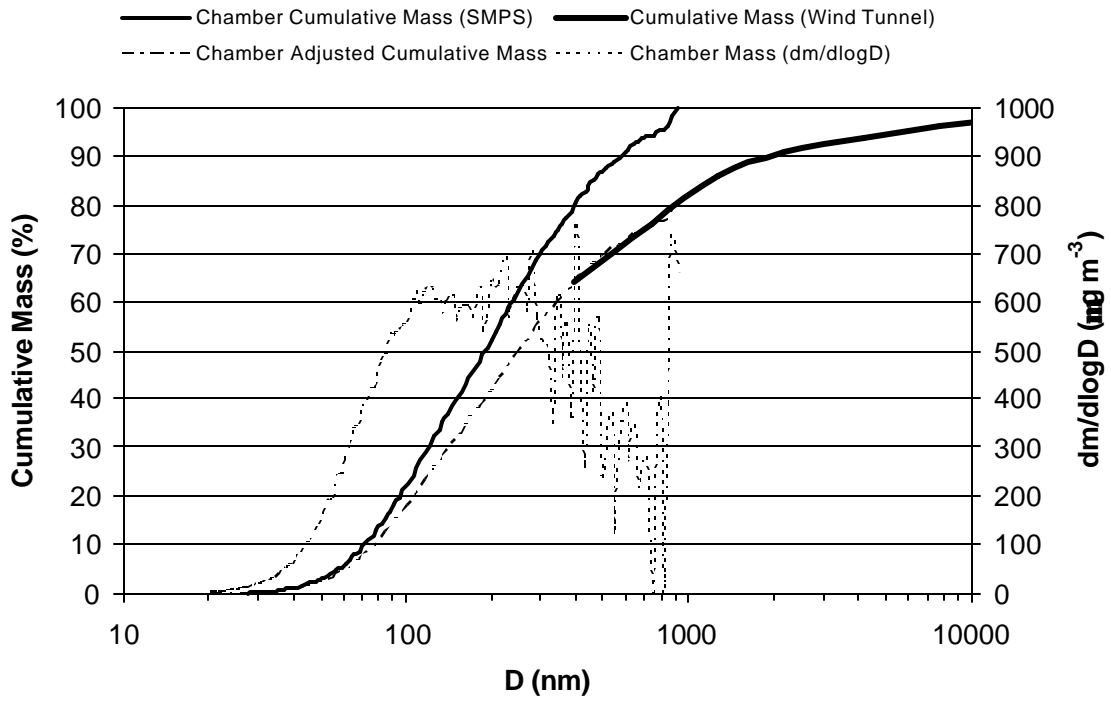


Figure 12. Cumulative particle mass and mass distributions determined by SMPS (size range 20 to 930 nm) for smoke in the exposure chamber under steady operation with a 45 s firing interval compared with cumulative mass distribution determined by cascade impactor from wind tunnel experiments with rice straw. The chamber distribution (adjusted cumulative mass) aligns with the wind tunnel distribution assuming the SMPS result accounts for 80% of total mass.

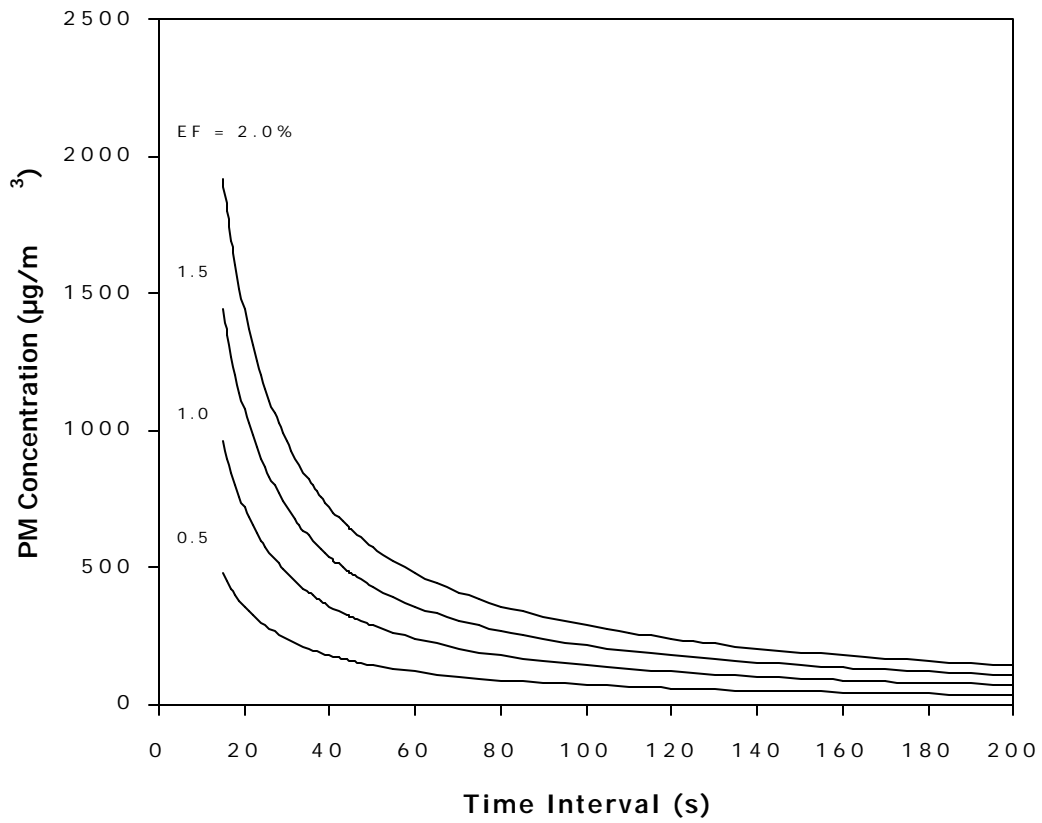


Figure 13. Estimated PM concentrations in the exposure chamber for different emission factors (EF, % dry matter) and firing time intervals.

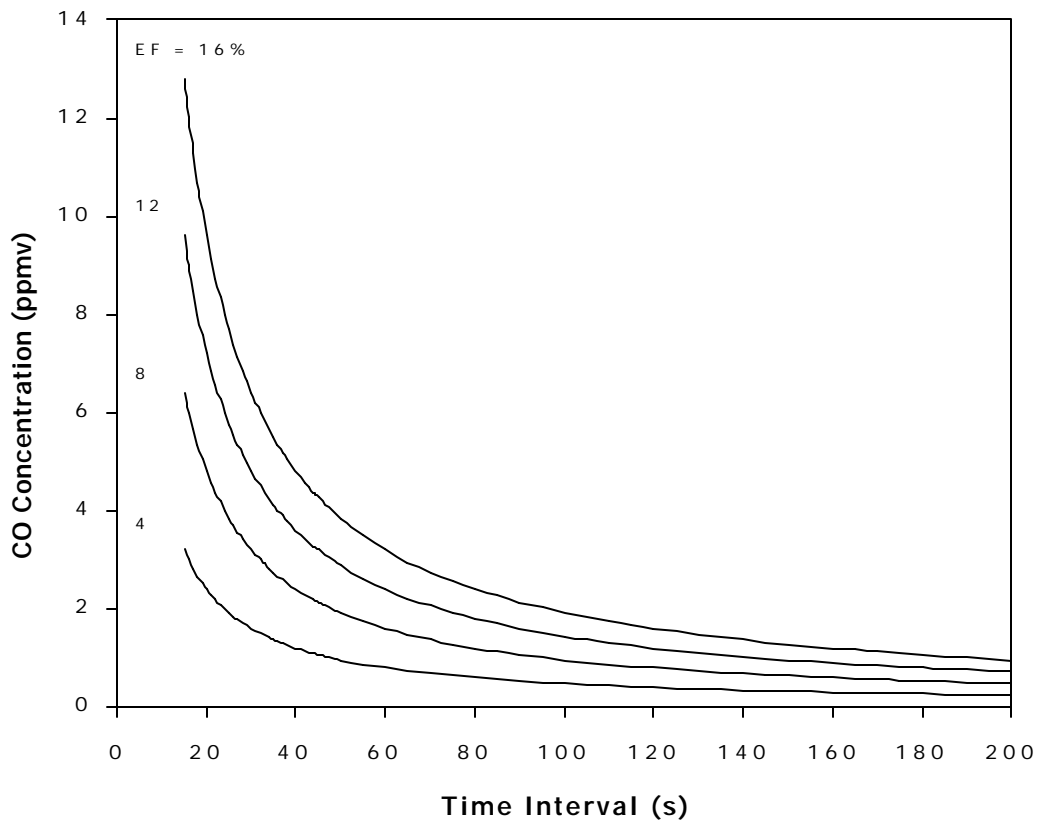


Figure 14. Estimated CO concentrations in the exposure chamber for different emission factors (EF, % dry matter) and firing time intervals.

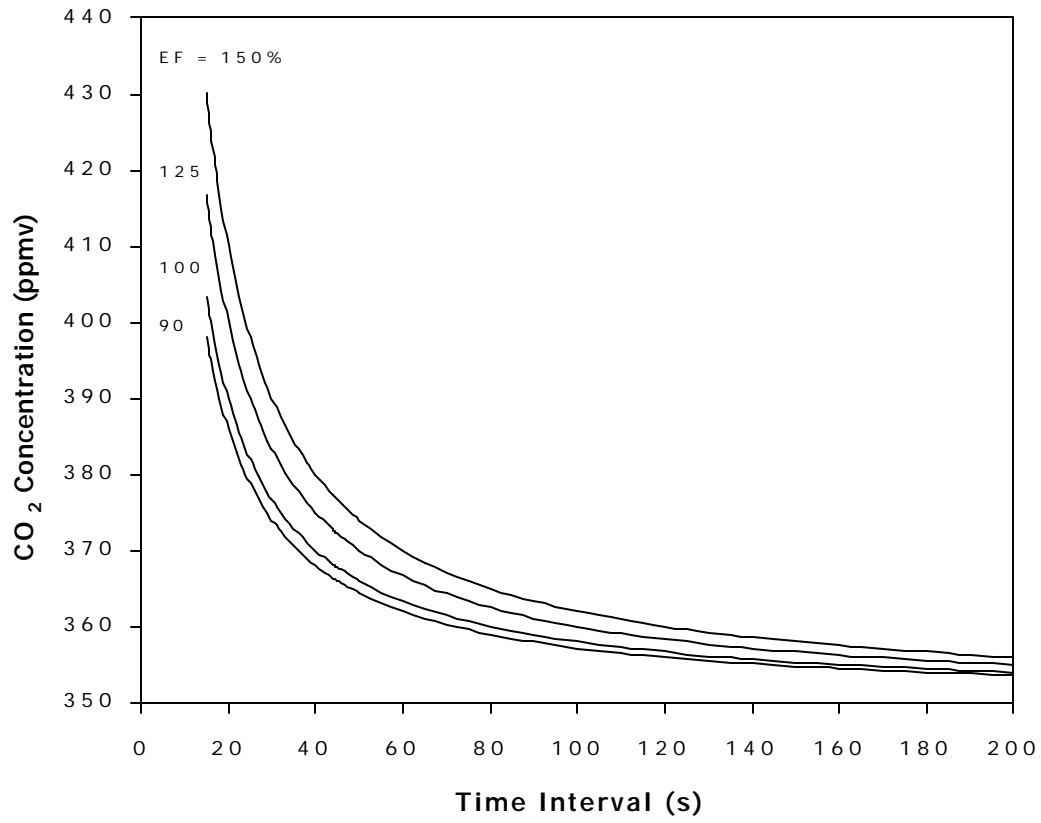


Figure 15. Estimated CO₂ concentrations in the exposure chamber for different emission factors (EF, % dry matter) and firing time intervals.